

Load Distribution on the Surface of Paraboloidal Reflector Antennas

M. Kron

DSIF Engineering Section

Wind pressure coefficients have been measured using wind tunnel models of parabolic reflectors. The application of this data and its conversion to useful form for structural deflection analysis within the "NASTRAN" Structural Analysis Computer Program and ultimately Root Mean Square (RMS) program is described in the following article.

I. Introduction

The determination of valid wind pressure distribution data is an important requirement for the design and analysis of large aperture antenna structures. These data can be acquired either from comprehensive full-scale field measurements or from scale-model wind tunnel test studies. The expense of current approaches to field measurement and questions of instrumentation accuracy and interpretations of results tend to make wind tunnel tests appear to be the more practical. Here, the problems of instrumentation and recording are substantially simplified with laboratory procedures and the scaling laws relating model and prototype are well known. Nevertheless, model tests entail questions of uncompensatable differences between wind tunnel and field environments. Therefore, it is necessary to recognize that model testing is an expedient and can reveal the necessity for compromises in the applicability of results.

The following discussion describes a procedure that is used to convert wind tunnel model pressure measurements into surface loading vectors for a prototype reflector of arbitrary size. Because of possible differences in wind tunnel and field environments and also in structural

topology, the derived loading vectors are useful primarily for preliminary design and analysis, or to substitute for the absence of more specific data.

II. Data Compilation

Pressures were measured at twenty-two locations on opposite halves of the convex and concave surfaces of the paraboloidal reflector (Fig. 1). The spacing was chosen to roughly represent equal areas per pressure orifice. (Ref. 1).

Table 1 presents tabulations of the resulting pressure coefficients C_p and the difference of the pressure coefficients ΔC_p for corresponding positions on the concave and convex surfaces of the reflector. The tabulations are arranged by position on the surface, while Fig. 2 defines the reflector angular attitudes.

The integral of the pressure coefficient over the reflector paraboloidal surfaces represents the major component of the force or moment on that body. These averaged experimental pressure coefficients were integrated by computer

using mathematical higher order curve fairing between data points.

Data for several surface configurations studied in (Refs. 1-3) using models with direct force-moment measuring devices and the conventional force (axial, normal, side) and moment (pitch, yaw, roll) coefficients were computed for each 5-deg increment of antenna elevation and azimuth orientations (Ref. 4).

III. Nomenclature (Fig. 3)

The position of the dish relative to the wind, is defined by the azimuth and elevation angles. The azimuth angle is the angle between the wind and the centerline of the paraboloidal reflector projected on the ground plane. The elevation angle is the angle between the reflector centerline and the ground plane. When both the azimuth and elevation angles are zero, the concave side of the reflector is directed symmetrically upwind. When the elevation angle is 90 deg, the antenna is pointed at the zenith.

The *body axis system* is a system which always moves with the dish and its axes define the directions of the axial, normal, and side force vectors. The origin is positioned at the reflector vertex and all moments are adjusted to apply at that point.

The forces and moments are in the form of the customary nondimensional aerodynamic coefficients. The force coefficients are defined as

$$\frac{\text{force}}{(\text{dynamic pressure}) \times (\text{reflector frontal area})} \quad (1)$$

and the moment coefficient as

$$\frac{\text{moment}}{(\text{dynamic pressure}) \times (\text{reflector frontal area})} \times \frac{\text{moment}}{(\text{reflector diameter})} \quad (2)$$

The dynamic pressure is defined as

$$\frac{1}{2} (\text{ambient static air density}) \times (\text{air velocity})^2$$

The force and moment sign conventions are tabulated as follows (refer to Fig. 3):

Axial force. Along the centerline and positive towards the concave surface at the reflector.

Normal force. Perpendicular to the centerline and positive in a vertical direction upwards when both the azimuth and elevation angles are zero.

Side force. Perpendicular to the centerline and positive to the right (viewed from the convex side) when the azimuth angle is zero and elevation angle is less than 90 deg.

Pitch moment. Positive for a pitch-up moment when azimuth angle is zero.

Yaw moment. Positive for a clockwise moment (viewed from above).

Roll moment. Positive for a clockwise moment when viewed from the convex side of a reflector.

IV. Discussion of Results

The use of an existing computer program used for polar contour plotting affords us the opportunity to input the pressure coefficient differences and allow the program to compute new pressure coefficients at selected points by interpolation from both radial and angular positions of the pressure taps and the topology of the surface panels of a paraboloidal reflector.

A computer program was written to compute the area associated with each node or target point on the reflector surface. In addition the algorithm computes the force from Eq. (1) and normalizes the force at each node according to the equation of the parabola. Components of the force vectors are computed from direction cosines and tabulated for each node, and for each set of input pressure tap data and antenna orientation. The program produces live load data for insertion into the NASTRAN statics program. Normally only loadings for zenith (Z loading) and horizon (Y loading) are used as input to the structural analysis program, since the displacements at any other position can be computed by a linear combination of both loadings. In the case of wind tunnel data, the data available for each position between 0 and 180 deg were treated independently in the NASTRAN program so that correction coefficients can eventually be developed for any other yaw and pitch angle. Since from Ref. 1 the moderately small influence of the ground plane effects can be extended to the pressure coefficients, therefore, force vectors may be computed for any antenna angular attitudes where the spherical sums of the yaw and pitch angles are equal to the pitch angle tested.

Table 2 provides a tabular summation of the forces computed for each case, using the pressure coefficients computed in Ref. 4. Table 3 contains the summation of forces for the same cases as computed using the wind pressure computer program.

Comparing the results of Tables 2 and 3 indicates results of the same order of magnitude. The lack of closer comparison is attributed to the wind tunnel anomalies and the manner in which a balance was used for resolving the force and moments. A correction factor was developed to relate the pressure coefficient readings more closely to the force-moment balance model readings.

Correction factor =

$$\frac{(C_{p(\text{normal})}^2 + C_{p(\text{axial})}^2)^{1/2}}{[(\sum \text{Force}_{(\text{normal}/\text{area})})^2 + (\sum \text{Force}_{(\text{axial}/\text{area})})^2]^{1/2}}$$

Table 3 also contains the summation of forces after application of the correction factor.

The output of the program consists of new live loadings of force vectors at surface panel connection points for input to the NASTRAN Structural Program. In all of the above calculations a dynamic pressure of 47.88 N/m² (1 lb/ft²) was used to compute the force vectors, which is

equivalent to 32.2-km/h (20 mph) wind velocity. The results of the rms program for each case appear in Table 4, and are best-fit rms with respect to rigid body motion.

The above discussion concludes Phase I of a broad program to investigate methods of attaining realistic wind data for paraboloidal reflectors, and the utilization of these data in present structural design analysis capabilities.

Future phases of the program would include:

- (1) Instrumenting an antenna with pressure taps to record pressure coefficients at panel connection points.
- (2) Correlating full size model results with wind tunnel data to determine confidence levels for larger antenna designs.
- (3) Relating pressure distribution data over reflector surfaces to direct axis forces-moments for use in antenna drive power requirements.
- (4) Developing thermal vs wind loading relationships from instrumenting full size models.
- (5) Relating various wind yaw angle and pitch angle field measurements to reference data to determine if linearity correction factors can be derived.

References

1. Fox, N. L., *Load Distribution on the Surface of Paraboloidal Reflector Antennas*, CP-4, July 1962 (JPL internal document).
2. Blaylock, R. B., *Aerodynamic Coefficients for a Model of a Paraboloidal Reflector Directional Antenna Proposed for a JPL Advanced Antenna System*, DP-6, May 1, 1964 (JPL internal document).
3. Schlichting, H., *Boundary Layer Theory*, McGraw-Hill, New York, 1960.
4. Levy, R., and Kurtz, D., "Compilation of Wind Tunnel Coefficients for Parabolic Reflectors," in *The Deep Space Network*, Space Programs Summary 37-63, Vol. II, pp. 36-42. Jet Propulsion Laboratory, Pasadena, Calif., May 31, 1970.

Table 1. Pressure coefficients on a thin paraboloidal solid surface

Focal-length-to-diameter ratio, 0.330 solid surface		Diameter Reynolds No., 2.7×10^6 0-deg yaw (azimuth) angle																			
		0-deg Pitch angle				60-deg Pitch angle				90-deg Pitch angle				120-deg Pitch angle				180-deg Pitch angle			
		R/D ^a	θ , ^a deg	Concave C_p	Convex C_p	ΔC_p	Concave C_p	Convex C_p	ΔC_p	Concave C_p	Convex C_p	ΔC_p	Concave C_p	Convex C_p	ΔC_p	Concave C_p	Convex C_p	ΔC_p			
0.468	15	+0.78	-0.55	+1.32	+0.29	-0.58	+0.87	+0.19	-0.36	+0.55	-0.41	-0.43	+0.02	-0.53	+0.42	-0.95					
	45	+0.78	-0.52	+1.30	+0.34	-0.63	+0.97	+0.11	-0.14	+0.25	-0.40	-0.42	+0.03	-0.53	+0.21	-0.75					
	75	+0.79	-0.55	+1.33	+0.38	-2.00	+2.38	-0.25	-0.27	+0.01	-0.38	-0.37	-0.01	-0.55	+0.08	-0.62					
	105	+0.81	-0.58	+1.39	+0.58	-3.76	+4.34	-0.34	-0.20	-0.14	-0.36	-0.10	-0.26	-0.54	+0.07	-0.61					
	135	+0.84	-0.60	+1.44	+0.73	-1.60	+2.32	-0.27	+0.29	-0.57	-0.35	+0.46	-0.81	-0.50	+0.06	-0.56					
	165	+0.90	-0.63	+1.52	+0.66	-1.14	+1.80	-0.24	+0.75	-0.99	-0.35	-0.35	+0.93	-1.28	+0.07	-0.59					
0.408	15	+0.94	-0.54	+1.47	+0.55	-0.60	+1.16	+0.17	-0.36	+0.53	-0.40	-0.49	+0.10	-0.52	+0.60	-1.12					
	45	+0.94	-0.55	+1.48	+0.59	-0.66	+1.25	+0.08	-0.22	+0.30	-0.38	-0.54	+0.16	-0.55	+0.47	-1.02					
	75	+0.95	-0.56	+1.50	+0.63	-1.39	+2.02	-0.33	-0.36	+0.03	-0.37	-0.44	+0.07	-0.54	+0.37	-0.91					
	105	+0.95	-0.59	+1.54	+0.69	-1.84	+2.53	-0.36	-0.28	-0.08	-0.35	-0.05	-0.30	-0.52	+0.33	-0.35					
	135	+0.97	-0.63	+1.60	+0.73	-0.73	+1.46	-0.31	+0.15	-0.46	-0.35	+0.54	-0.89	-0.51	+0.31	-0.82					
	165	+0.99	-0.66	+1.65	+0.69	-0.51	+1.19	-0.27	+0.50	-0.77	-0.33	-0.33	+0.93	-1.26	+0.32	-0.83					
0.326	15	+0.98	-0.55	+1.53	+0.69	-0.64	+1.33	-0.03	-0.34	+0.32	-0.38	-0.53	+0.15	-0.52	+0.77	-1.29					
	45	+0.99	-0.53	+1.52	+0.71	-0.69	+1.40	-0.06	-0.30	+0.24	-0.38	-0.61	+0.23	-0.53	+0.72	-1.24					
	75	+0.98	-0.57	+1.55	+0.73	-0.97	+1.70	-0.34	-0.40	+0.06	-0.36	-0.48	+0.12	-0.50	+0.63	-1.13					
	105	+0.99	-0.60	+1.59	+0.78	-0.88	+1.66	-0.38	-0.31	-0.06	-0.36	-0.07	-0.29	-0.52	+0.58	-1.10					
	135	+1.01	-0.64	+1.64	+0.76	-0.63	+1.39	-0.35	-0.01	-0.34	-0.37	-0.37	+0.44	-0.81	+0.58	-1.10					
	165	+1.01	-0.66	+1.67	+0.74	-0.43	+1.17	-0.30	+0.60	-0.60	-0.34	-0.34	+0.80	-1.14	+0.56	-1.07					
0.206	15	+1.00	-0.54	+1.54	+0.79	-0.73	+1.52	-0.22	-0.34	+0.13	-0.37	-0.61	+0.24	-0.51	+0.84	-1.35					
	75	+1.01	-0.56	+1.57	+0.79	-0.83	+1.62	-0.35	-0.42	+0.07	-0.36	-0.48	+0.12	-0.53	+0.82	-1.35					
	105	+1.01	-0.60	+1.61	+0.79	-0.73	+1.52	-0.37	-0.34	-0.03	-0.36	-0.18	-0.18	-0.52	+0.79	-1.30					
	165	+1.02	-0.63	+1.65	+0.81	-0.29	+1.10	-0.32	+0.00	-0.33	-0.36	-0.36	+0.59	-0.95	+0.82	-1.32					

^aSee Fig. 1 for definitions of R/D and θ .

Table 2. Summation of wind forces computed from force-moment balance model

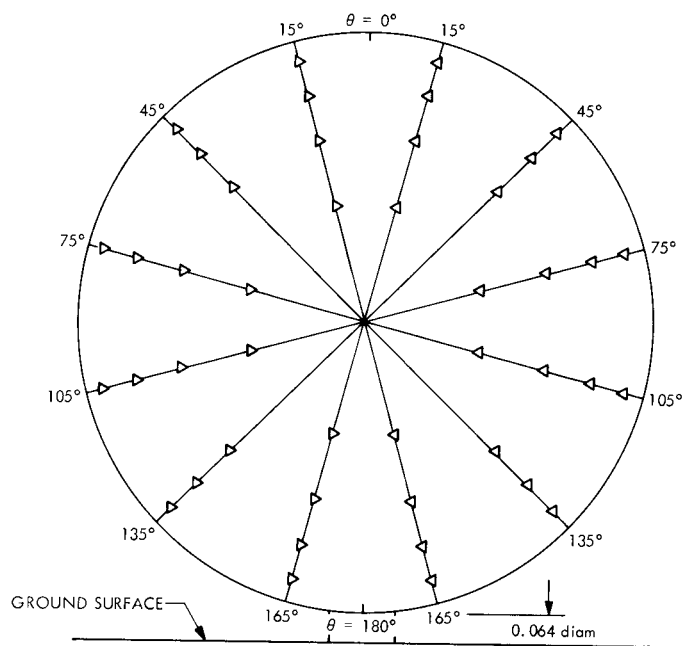
Case No.	Σ Force (side) $\times 4.448$ N	Σ Force (normal) $\times 4.448$ N	Σ Force (axial) $\times 4.448$ N
1	-5.67	-90.79	4315.44
2	-31.21	-221.30	5197.82
3	-19.86	434.10	0.0
4	0	612.84	-1702.34
5	5.67	-85.12	-2726.59

Table 3. Summation of wind forces computed from wind pressure distribution program with corrections

Fig. 2 Case No.	Σ Force (side) $\times 4.448$ N		Σ Force (normal) $\times 4.448$ N		Σ Force (axial) $\times 4.448$ N	
	Computed	Corrected	Computed	Corrected	Computed	Corrected
1	915.82	1027.55	-40.35	-45.27	3851.30	4321.16
2	1064.39	1274.07	-98.39	-117.77	4217.95	5048.87
3	-59.45	-68.72	271.36	-313.69	-259.38	-299.84
4	-135.24	-407.34	249.10	750.29	-593.73	-1788.31
5	-560.71	-604.43	-60.40	-65.11	-2528.74	-2725.98

Table 4. Summation of best-fit rms 26-m az-el wind loading

Case	rms $\times 2.54$ cm
1	0.0057
2	0.0116
3	0.0025
4	0.0094
5	0.0034



LOOKING INTO CONCAVE FACE AT ZERO PITCH AND YAW ANGLES

- ◁ PRESSURE TAP ON CONCAVE SURFACE
- ▷ PRESSURE TAP ON CONVEX SURFACE
- θ = ANGULAR POSITION OF PRESSURE TAPS
- R/D = RADIAL POSITION OF PRESSURE TAPS

Fig. 1. Pressure tap locations on model

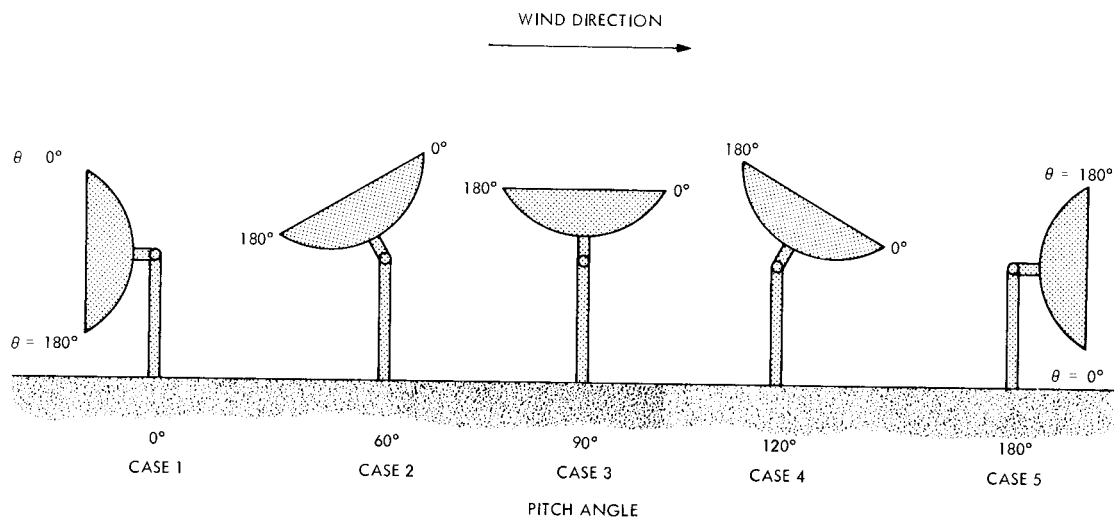


Fig. 2. Paraboloidal reflector antenna model attitudes

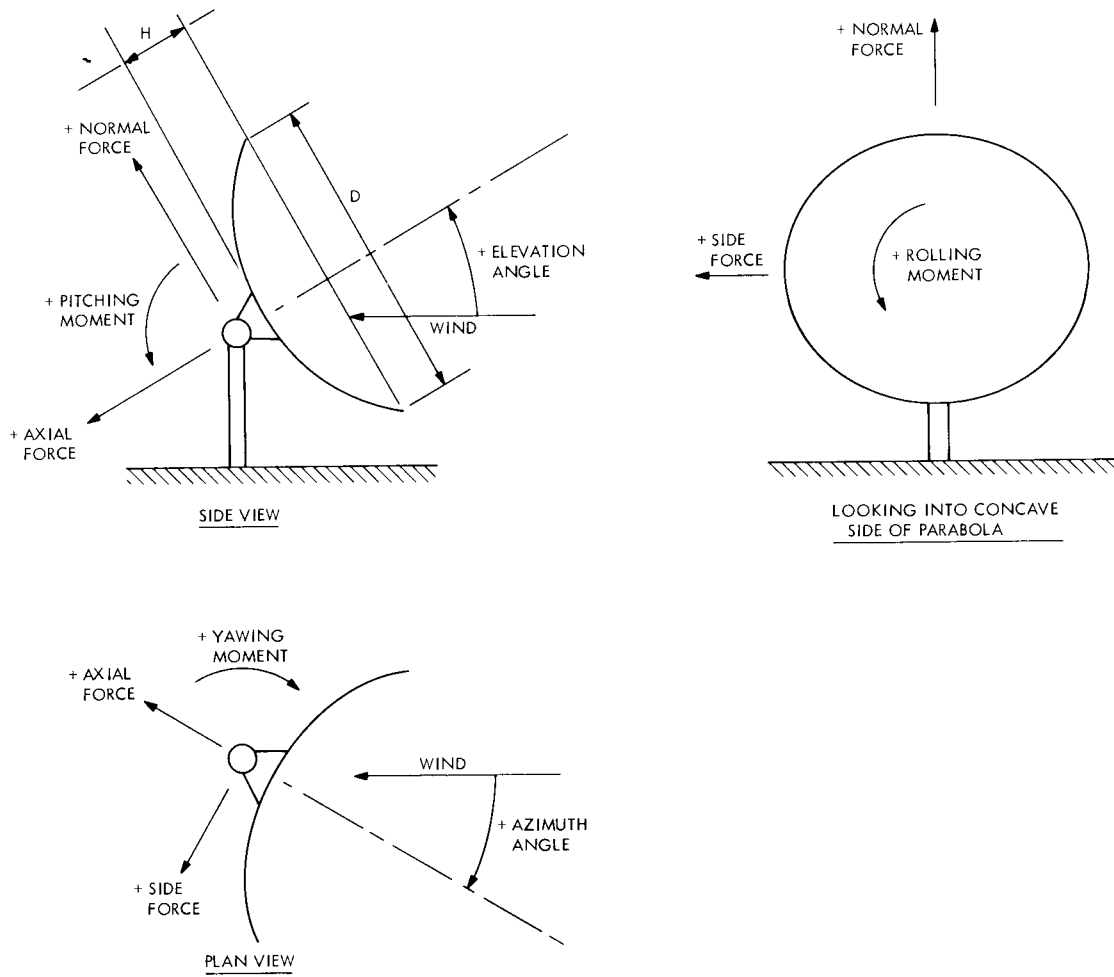


Fig. 3. Nomenclature for force-moment tabular